Dissociation of $SO_4^{2-}(H_2O)_n$ Clusters, $n = 3-17$

Richard L. Wong and Evan R. Williams*

Department of Chemistry, University of California, Berkeley, California 94720

Received: August 29, 2003; In Final Form: October 8, 2003

The dissociation pathways and energetics of $SO_4^{2-}(H_2O)_n$ for $n = 3-17$ were studied with use of a combination of blackbody infrared radiative dissociation (BIRD), sustained off-resonance irradiation collisional activated dissociation (SORI-CAD), infrared multiphoton dissociation (IRMPD), and double resonance experiments. For $n = 7-17$, the loss of a single water molecule is the only process observed. For $n = 6$, loss of a single water molecule is the dominant reaction (>90%), but some charge separation products are observed. In contrast, loss of a water molecule from the $n = 5$ cluster is small (<10%) and two charge separation pathways are the dominant processes observed. For both $n = 3$ and 4, charge separation is the only process that occurs at low internal energy. For both $n = 5$ and 6, the branching ratio of water loss to charge separation increases with increasing internal energy deposited into the clusters. This demonstrates that the water loss process is entropically favored over the charge separation process. Rate constants for loss of a water molecule from $n = 6-17$ clusters were measured with BIRD at 21 °C. A large increase is observed between $n = 6$ and 7, indicating that the seventh water molecule may go into an outer solvation shell or it may disrupt an unusually stable arrangement of water molecules at $n = 6$. The $n = 12$ cluster is more stable than either $n = 11$ or 13. This "magic" number hydrate is consistent with filling of a shell structure at $n = 12$. One such structure in which all 12 water molecules are symmetrically bonded to SO_4^{2-} is identified as a low-energy structure at the B3LYP 6-31 G**++ level, although this structure is entropically disfavored compared to those where one or two water molecules occupy a second solvation shell.

Introduction

Multiply charged anions, such as sulfate (SO_4^{2-}), play an important role in chemistry and biochemistry. Although SO_4^{2-} exists in protic solvents, like water and methanol, the bare dianion has not been observed in the gas phase, where calculations indicate that it is electronically unstable with respect to electron detachment.[1,2] For electron detachment from a multiply charged anion to occur, a barrier due to the combined short-range molecular binding and the long-range Coulomb repulsion between the anion and departing electron must be overcome. Thus, multiply charged ions may be metastable even if they are electronically unstable.[3−13] Simons and co-workers calculated that the lifetime of SO_4^{2-} with respect to electron loss is 1.6×10^{-10} s using a one-dimensional tunneling modeling with a potential barrier of 5.88 eV.[13] Reducing the barrier to 4.37 eV results in a change in the lifetime by less than 1 order of magnitude.[13]

In contrast, gaseous $SO_4^{2-}(H_2O)_n$ clusters can be easily produced by using electrospray ionization as first demonstrated by Blades and Kebarle.[14] The surrounding water molecules stabilize the clusters from electron detachment.[14−17] Blades and Kebarle generated clusters as small as $n = 4$, and observed a small signal for the $n = 2$ cluster generated by collisional activation dissociation (CAD) of the $n = 4$ cluster.[14] Using photodetachment photoelectron spectroscopy (PES), Wang and co-workers quantitatively showed that each additional water ligand on $SO_4^{2-}(H_2O)_n$ has a stabilizing effect against electron detachment, with $n = 3$ being the smallest cluster observed in their experiment.[16,17] The measured adiabatic electron detachment energy of $SO_4^{2-}(H_2O)_n$ increases from 0.4 eV for the $n = 3$ cluster to 0.92 eV for the $n = 4$ cluster and to 5.73 eV for the $n = 40$ cluster. By extrapolating the stabilizing effect of each water molecule, clusters at both $n = 1$ and 2 were predicated to be electronically unstable by −0.9 and −0.2 eV, respectively, in excellent agreement with theoretical values of −0.91 and −0.22 eV.[15] Thus, Wang and co-workers concluded that three water molecules is the minimum needed to stabilize SO_4^{2-}. On the other hand, the observation of the $n = 2$ cluster by Blades and Kebarle indicates that this dianion cluster has a sufficiently long lifetime to be detected by mass spectrometry.

Because of the short lifetime of SO_4^{2-} (1.6×10^{-10} s) with respect to electron detachment,[13] the $SO_4^{2-}(H_2O)_n$ clusters observed in electrospray ionization are almost certainly formed by evaporation of water molecules from larger clusters and droplets, not by condensation of water molecules on bare SO_4^{2-}. Condensation of water molecules on minimally hydrated divalent ions often results in charge separation dissociation via proton transfer.[18−21] For example, Spears et al. demonstrated that $Ca^{2+}(H_2O)_2$ cannot be formed by association of a water molecule with $Ca^{2+}(H_2O)$ since the resulting cluster spontaneously dissociates to $CaOH^+$ and H_3O^+ when the second hydration occurs (reaction 1).[18,19] Even though $Ca^{2+}(H_2O)$ is

$$Ca^{2+}(H_2O) + H_2O \rightarrow CaOH^+ + H_3O^+ \qquad (1)$$

easily produced from bare Ca^{2+} by adding water, the charge separation channel for $Ca^{2+}(H_2O)_2$ lies notably lower in energy than the dehydration channel (loss of a water molecule). Thus,

* Address correspondence to this author. Phone: (510) 643-7161. E-mail: williams@cchem.berkeley.edu.

10.1021/jp036583r CCC: $25.00
Published on Web 11/15/2003

the addition of a second water molecule results in spontaneous dissociation by charge separation dissociation. Therefore, electrospray ionization appears to be an ideal method for producing hydrated divalent ions, such as $SO_4^{2-}(H_2O)_n$ clusters.

Blades and Kebarle studied the dissociation pathways of $SO_4^{2-}(H_2O)_n$, $n = 4$ and 14, using CAD, and found that the $SO_4^{2-}(H_2O)_{14}$ cluster dissociates primarily by dehydration (reaction 2),[14] whereas $SO_4^{2-}(H_2O)_4$ undergoes intraligand

$$SO_4^{2-}(H_2O)_{14} \rightarrow SO_4^{2-}(H_2O)_k + (14 - k)\, H_2O \qquad (2)$$

proton transfer followed by charge separation dissociation (reaction 3).

$$SO_4^{2-}(H_2O)_4 \rightarrow HSO_4^{-}(H_2O) + OH^{-}(H_2O)_2 \qquad (3)$$

From results of PES experiments, Wang and co-workers concluded that both electrons in $SO_4^{2-}(H_2O)_n$ clusters, $n \geq 4$, stay close to the sulfate and that neither charge transfer nor proton transfer to water occurs at room temperature.[15-17] Calculations showed that the structure of SO_4^{2-} remains structural unperturbed with minimal charge transfer to the surrounding water molecules for all $n = 1-6$ clusters. Thus, proton transfer observed in the CAD experiment must occur at or near the transition state of an activated cluster.

Interactions between SO_4^{2-} and water molecules in aqueous solution have been studied with use of X-ray diffraction.[22-26] The number of first shell water molecules that surrounds SO_4^{2-} is reported to be between 6 and 8,[22,24-26] although as many as 11 have been reported with use of a different model to interpret the data.[23] Blades and Kebarle deduced that 7 water molecules complete the first solvation shell of SO_4^{2-} based on observation of a "magic" number cluster ($n = 7$) in their CAD experiment.[14] Cannon and co-workers have performed molecular dynamic calculations and concluded that there are 13 water molecules in the first solvation shell of SO_4^{2-}.[27] Wang and co-workers reported that, as the number of water molecules increases above $n \sim 13$ for the $SO_4^{2-}(H_2O)_n$ clusters, a PES spectral feature at low binding energy gradually diminishes, while a new signal appears at high binding energy.[15-17] The low binding energy signal was attributed to SO_4^{2-} because the signal appears in spectra of smaller clusters. The new signal was attributed to ionization of water molecules. From these results, Wang and co-workers concluded that SO_4^{2-} is in the center of the water clusters, and that the first solvation shell of SO_4^{2-} is filled around $n \sim 12$. Jungwrith and co-workers recently reported results from classical and Car−Parrinello molecular dynamics for $SO_4^{2-}(H_2O)_{13}$ and showed that SO_4^{2-} prefers to be situated in the center of the cluster.[28]

Here, the dissociation pathways of $SO_4^{2-}(H_2O)_n$ for $n = 3-17$ are investigated by using blackbody infrared radiative dissociation (BIRD), infrared multiphoton dissociation (IRMPD) with a cw-CO_2 laser, and sustained off-resonance irradiation collisional activation dissociation (SORI-CAD). The energy dependence of competing dissociation pathways is studied by using these different activation methods from which information about the energetics and transition state entropies are obtained. Rate constants for loss of water from $n = 6-17$ clusters are measured and provide evidence for shell structures of water molecules surrounding SO_4^{2-}.

Experimental Section

Mass Spectrometry. All experiments are performed on a 2.7-Tesla Fourier transform ion cyclotron resonance (FT-ICR) mass spectrometer.[29] Ions are guided through five stages of differential pumping into the ion cell in the center of the magnetic field via a series of electrostatic lenses. Ion trapping and thermalization is enhanced by using nitrogen gas that is introduced through a piezoelectric pulsed valve to a pressure of $\sim 2 \times 10^{-6}$ Torr. Ions are isolated by using a combination of frequency sweep, SWIFT, and single-frequency waveforms. All BIRD experiments are performed at room temperature (~21 °C) and at a base pressure in the ion cell of 5×10^{-10} Torr. IRMPD experiments are conducted with a 28 W continuous wave CO_2 laser (Model No. 48-2-28W, Synrad Inc., Bothell, WA) at full power. The laser beam is guided toward the ion cell by a series of mirrors, and enters the vacuum system by passing through a ZnSe window mounted on the rear flange of the vacuum chamber. According to Synrad, Inc's specification and the total beam path length, the beam diameter is ~12.7 mm in the center of the ion cell. Thus, the photon power density experienced by the trapped ions is ~22 W/cm^2. SORI-CAD experiments are done by applying a frequency 2000 Hz lower than the resonance frequency of the targeted ions for 0.1−0.6 s with the ion cell maintained at a pressure of $\sim 2 \times 10^{-8}$ Torr by introducing N_2-(g) through a variable leak valve.

$SO_4^{2-}(H_2O)_n$ clusters are produced with use of nanoelectrospray from 1×10^{-4} M $MgSO_4$ solution in a water/methanol mixture (80:20 by volume). $MgSO_4$ was purchased from Fisher Scientific (Fair Lawn, NJ). Nanoelectrospray needles are made from 1.0 mm o.d. borosilicate capillaries that are pulled to an i.d. of ~ 4 μm at one end with a micropipet puller (Sutter Instruments Inc., Novato, CA).

First-order dissociation rate constants for loss of a water molecule were obtained by fitting a plot of $\log_e [SO_4^{2-}(H_2O)_n]/\{[SO_4^{2-}(H_2O)_n] + [SO_4^{2-}(H_2O)_{n-1}]\}$ versus time. Between 30 and 50 scan averages were used to obtain the mass spectra for these data.

Modeling. Low-energy structures of $SO_4^{2-}(H_2O)_n$, $n = 4-10$, are identified by using an internal coordinate Monte Carlo search with 4000 iterations followed by a molecular mechanics energy minimization with the MMFFs force field in the Maestro3.0 suite of programs (Schrödingner Inc., Portland, OR). Due to the large translational degrees of freedom, low-energy structures of $SO_4^{2-}(H_2O)_n$, $n = 11-13$, are identified by using molecular dynamics (MMFFs) at 400 K for 2000 ps at 1.0 fs time steps. Structures are saved every 1.0 ps and are subsequently energy minimized. A similar molecular dynamics/multiple minimization method is also performed for the $n = 11-13$ clusters at 1000 K for 1000 ps at 0.5 fs time steps while constraining the sulfate−water distance to 10 Å or less. The lowest energy structures identified at the two temperatures are the same. For the $n = 12$ cluster, both the lowest energy structure found with the molecular dynamics simulation as well as a symmetrical structure are energy optimized at the B3LYP/6-31 G**++ level with Jaguar 4.0 (Schrödingner Inc., Portland, OR).

Results and Discussion

A typical electrospray spectrum obtained from a 10^{-4} M $MgSO_4$ water/methanol (80:20 by volume) solution under gentle source and ion introduction conditions that promote formation of solvated ions is shown in Figure 1a. Ions corresponding to $SO_4^{2-}(H_2O)_n$, $HSO^{-}(H_2O)_x$, and $OH^{-}(H_2O)_y$ clusters are produced (Figure 1a). In these experiments, $n = 5$ is the smallest $SO_4^{2-}(H_2O)_n$ cluster observed. In contrast, Wang and co-workers observed clusters as small as $n = 3$.[15] As will be presented later, the loss of a water molecule from $SO_4^{2-}(H_2O)_4$ is a higher energy process but is entropically favored compared to the

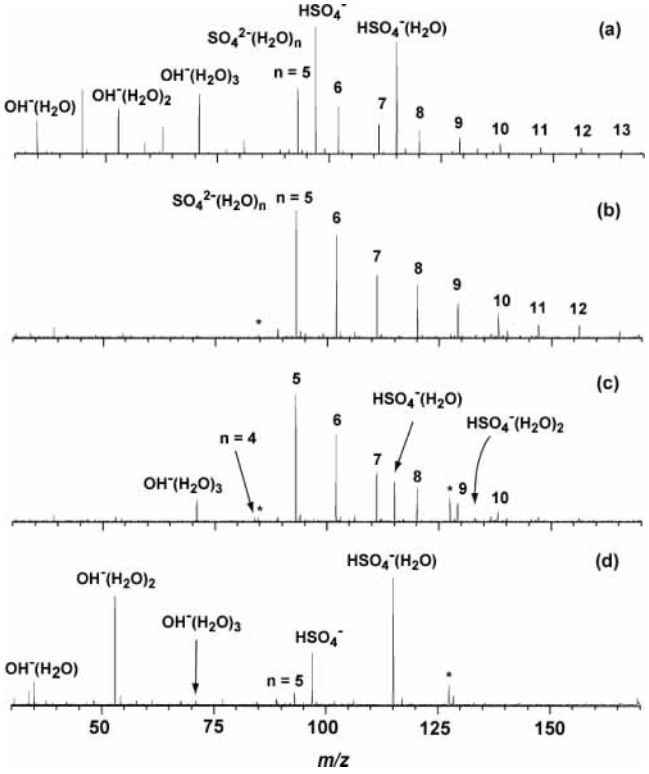

Figure 1. Mass spectra from (a) electrospray ionization of a 10^{-4} M $MgSO_4$ water/methanol solution (80:20 volume), (b) after isolation of $SO_4^{2-}(H_2O)_n$, $n \geq 5$ at zero reaction time, (c) with BIRD (3 s, 21 °C), and (d) with IRMPD (5.0 s, 28 W CO_2 laser). Asterisks (*) indicate known noise peaks.

alterative charge separation reaction. The lower energy processes are favored in this experiment due to the gentle source and ion introduction conditions and the longer measurement time frame of FT-ICR MS.

To determine general fragmentation pathways of the $SO_4^{2-}(H_2O)_n$ clusters ($n \geq 5$), these ions were isolated with SWIFT and single-frequency waveforms (Figure 1b), and dissociated with blackbody infrared radiative dissociation (BIRD) (Figure 1c) and infrared multiphoton dissociation (IRMPD) (Figure 1d). $SO_4^{2-}(H_2O)_4$ is the smallest doubly charged cluster produced. This ion dissociates exclusively by a charge separation reaction to produce two singly charged fragment ions with BIRD or IRMPD.

$SO_4^{2-}(H_2O)_n$, $n = 6-17$. To obtain dissociation pathways and rate constants for $SO_4^{2-}(H_2O)_n$ clusters, clusters corresponding to $n = 6-17$ are individually isolated and dissociated with BIRD at 21 °C. Double resonance experiments are performed to elucidate the dissociation pathways. For example, the $n = 13$ cluster is isolated (Figure 2a) and dissociated with BIRD for 0.2 s (Figure 2b). The $n = 12$ cluster (loss of a water molecule) is the only product ion observed. The isotope peaks confirm these ions are doubly charged. At a reaction time of 0.8 s, the relative abundance of the $n = 12$ cluster increases, and the signal for the $n = 11$ cluster also appears (Figure 2c). Applying an ejection frequency corresponding to $n = 12$ for the duration of the reaction eliminates both $n = 11$ and 12 clusters (Figure 2d). The double resonance experiment demonstrates that the $n = 13$ cluster dissociates exclusively by sequential loss of water molecules. Using double resonance experiments, clusters of $n = 7-17$ were determined to dissociate solely via loss of a single water molecule (dehydration).

A 4.0-s BIRD spectrum of $n = 6$ shows a large peak at $n = 5$ and some charge separation products: $HSO_4^-(H_2O)_x$ and

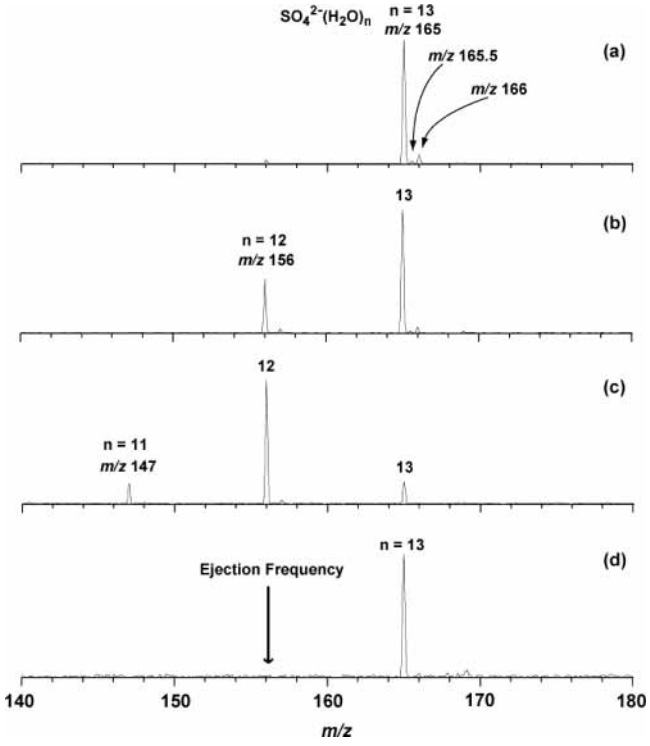

Figure 2. Mass spectra of $SO_4^{2-}(H_2O)_{13}$ (a) after isolation at zero reaction time and (b−d) with BIRD (0.2 s, 21 °C (b); 0.8 s, 21 °C (c); and 0.8 s, 21 °C (d)) while continuously applying a RF waveform at the frequency corresponding to $SO_4^{2-}(H_2O)_{12}$, *m/z* 156.

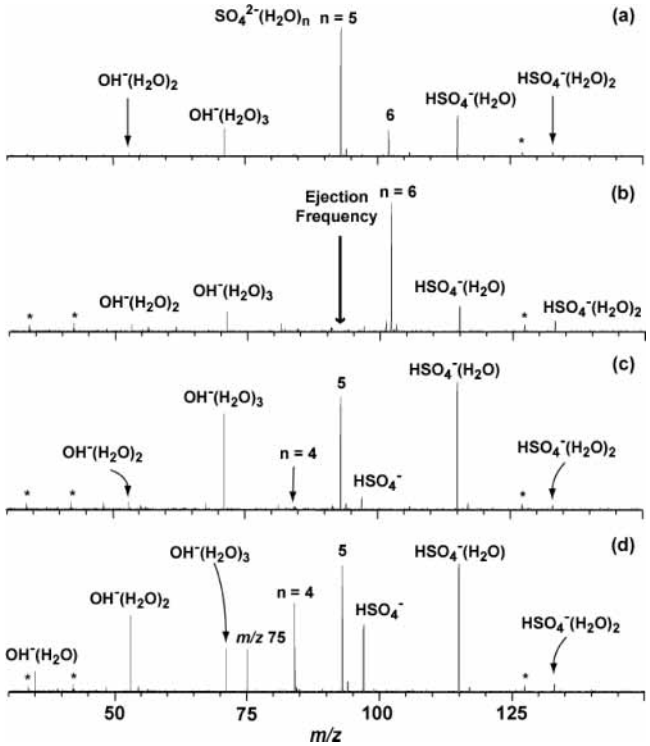

Figure 3. Dissociation spectra of (a) $SO_4^{2-}(H_2O)_6$ with BIRD (4.0 s, 21 °C), (b) $SO_4^{2-}(H_2O)_6$ with BIRD (4.0 s, 21 °C) continuously ejecting $SO_4^{2-}(H_2O)_5$, (c) $SO_4^{2-}(H_2O)_5$ with BIRD (4.0 s, 21 °C), and (d) $SO_4^{2-}(H_2O)_5$ with SORI-CAD. Asterisks (*) indicate known noise peaks.

$OH^-(H_2O)_y$ (Figure 3a). Applying an ejection frequency corresponding to $n = 5$ eliminates most, but not all, charge separation products (Figure 3b). The $n = 5$ ion in this double resonance experiment is ejected from the ion cell in less than

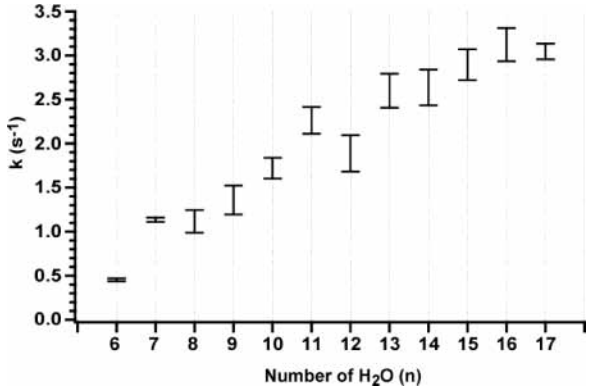

Figure 4. Rate constants for loss of a water molecule from $SO_4^{2-}(H_2O)_n$, $n = 6-17$, with BIRD at 21 °C as a function of n. The error bars represent ± one standard deviation of the measured rate constant.

0.001 s. On the basis of the dissociation rate constants of the $n = 5$ and 6 clusters and the ion ejection time, we conclude that less than 1% of the total ion intensity due to charge separation reactions in Figure 3b comes from the $n = 5$ ion before it is ejected from the cell. Thus, the two reaction pathways for the $n = 6$ ion are given below (reactions 4a and b).

$$SO_4^{2-}(H_2O)_6 \rightarrow SO_4^{2-}(H_2O)_5 + H_2O \quad (4a)$$

$$\rightarrow HSO_4^{-}(H_2O)_2 + OH^{-}(H_2O)_3 \quad (4b)$$

A branching ratio for reactions 4a and 4b of 14:1 is obtained.

The BIRD rate constants for dehydration for $SO_4^{2-}(H_2O)_n$, $n = 6-17$, were obtained by fitting dissociation data measured as a function of time. These data as a function of cluster size are shown in Figure 4. The error bars in Figure 4 represent ± one standard deviation determined from fitting the kinetic data. Rate constants for dehydration were not obtained for $n \leq 5$ because charge separation is the dominant dissociation reaction for these ions. It is important to note that the internal energy distributions of the ions in this experiment are Boltzmann-like, but are depleted at the higher energies. The extent of the depletion depends on a number of factors, including the threshold dissociation energy, the infrared photon absorption and emission rate, etc.[30]

The dehydration rate constants generally increase with the number of water molecules in the clusters, consistent with the lower binding energy and larger infrared radiative absorption cross section with increasing cluster size. Two clusters appear to deviate from the general trend. The dissociation rate constant for the $n = 12$ cluster is noticeably smaller than those for the $n = 11$ and 13 clusters. And a significant increase in the dissociation rate constant occurs between $n = 6$ and 7, with the measured rate constant for $n = 7$ marginally greater than that for $n = 8$.

These kinetics data are interesting in that the number of water molecules that complete the first solvation shell for $SO_4^{2-}(H_2O)_n$ is still not well-known. Results from X-ray diffraction in solution indicate that there are ca. 6−8 water molecules in the first solvation shell,[22,24−26] although as many as 11 have been reported with use of a different model to fit the data.[23] Previous CAD results suggested that 7 water molecules complete the first solvation shell.[14] Computational results indicate that there are 13 inner shell water molecules,[27] and results from PES suggest approximately 12 water molecules.[16,17]

The anomalously weak $n = 7$ measured here is consistent with filling the first solvation shell of closely interacting water molecules at $n = 6$. We define an inner shell water molecule as one that forms one or two hydrogen bonds directly with SO_4^{2-}. The seventh water molecule may go into a second solvation shell or it may still be in the first solvation shell, but simply disrupts the stable arrangement of water molecules at $n = 6$. The lower dissociation rate constants for the $n = 12$ cluster versus $n = 11$ and 13 indicate a stronger water binding interaction for this ion (Figure 4). This is consistent with a completed solvation shell structure at $n = 12$, with the 13th water molecule going into a higher solvation shell. It is also possible that the stability for the $n = 12$ cluster may be due to a specifically stable network of water molecules around the ion.

Structures. To obtain information about structures that may explain the unusual kinetic data for $n = 6$, 7, and 12, molecular modeling was performed on the $n = 4-13$ clusters with the MMFFs force field. The lowest energy structure obtained for $n = 4$ is one in which four equivalent water molecules each form two hydrogen bonds to two oxygen atoms in SO_4^{2-} such that each oxygen in SO_4^{2-} is involved in two hydrogen bonds with two water molecules. This is the same structure as that reported by Wang and co-workers, who investigated the structures of $n = 1-6$ at the B3LYP/TZVP+ level.[15] Similarly, the structure for $n = 5$ is one in which all five water molecules each form two hydrogen bonds to SO_4^{2-}. A slightly higher energy structure (+10 kJ/mol) in which one water molecule forms one hydrogen bond to SO_4^{2-} and one to another water molecule is identified. The latter structure is the same structure identified by Wang and co-workers as the lowest energy structure with density functional theory.

For $n = 6$, we find only one low-energy structure within 12 kJ/mol. Each water molecule in this structure forms two hydrogen bonds to SO_4^{2-} (Figure 5a). By comparison, the structure identified by Wang and co-workers at the B3LPY/TZVP+ level has three water molecules with two hydrogen bonds to SO_4^{2-} as in the mechanics structure, but three other water molecules each has only one hydrogen bond to SO_4^{2-} and two hydrogen bonds to two adjacent water molecules. In this structure, only one oxygen atom in SO_4^{2-} has three hydrogen bonds to water versus the mechanics structure in which all four oxygen atoms each has three hydrogen bonds to water. The results for $n = 4-6$ indicate that the mechanics calculations may overvalue the stabilizing effects of three hydrogen bonds to oxygen in SO_4^{2-}.

For $n = 7$, there are five structures that are within 12 kJ/mol of the lowest energy structure. The lowest energy structure is similar to that for $n = 6$ with the seventh water molecule located in an outer solvation shell with two hydrogen bonds to two water molecules (Figure 5b). Four of the remaining structures have all seven water molecules directly interacting with SO_4^{2-}. In these structures, three water molecules remain in the very stable arrangement as identified for $n = 6$, but there are only three oxygen atoms in SO_4^{2-} available to form hydrogen bonds with the remaining four water molecules. One such structure, in which five water molecules each has two hydrogen bonds to SO_4^{2-} and two water molecules each has a single hydrogen bond to SO_4^{2-} and a single hydrogen bond to an adjacent water molecule, is shown in Figure 5c.

The results from the mechanics calculations indicate only one stable structure for $n = 6$ but several stable structures for $n = 7$, both with all seven water molecules in the first solvation shell and with the seventh water molecule in the second solvation shell. These structures are consistent with the unusually rapid dissociation observed for the $n = 7$ structure.

For $n = 11-13$, the number of low-energy structures identified by molecular dynamic simulation is significantly

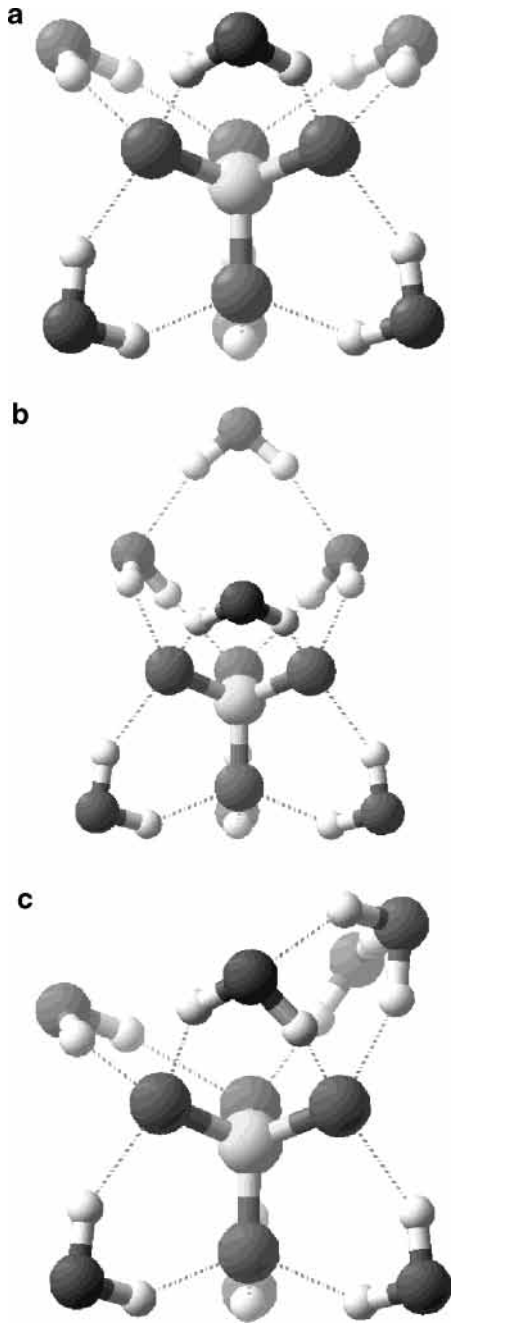

Figure 5. Molecular mechanics structures of (a) $SO_4^{2-}(H_2O)_6$ (lowest energy structure) and (b, c) $SO_4^{2-}(H_2O)_7$ (lowest and second lowest energy structure, respectively).

greater with over 30 low-energy structures identified for each. No structure with all first solvation shell water molecules was found within 12 kJ/mol of the lowest energy structure. For instance, the lowest energy structure for $n = 12$ identified by molecular mechanics is one in which two water molecules are in the second solvation shell (Figure 6a). We also input a symmetrical structure (Figure 6b) in which each of the 12 water molecules forms a single hydrogen bond to SO_4^{2-} and two hydrogen bonds to two adjacent water molecules. After energy minimization, this structure is 17 kJ/mol higher in energy than the lowest energy structure identified by mechanics. However, at the B3LYP/6-31 G**++ level (full geometry optimization), this symmetrical structure (Figure 6b) is 1 kJ/mol lower in energy than the structure identified by the mechanics calculation (Figure 6a). After zero point energy and temperature correction (25 °C), the free energy of the symmetrical structure (Figure

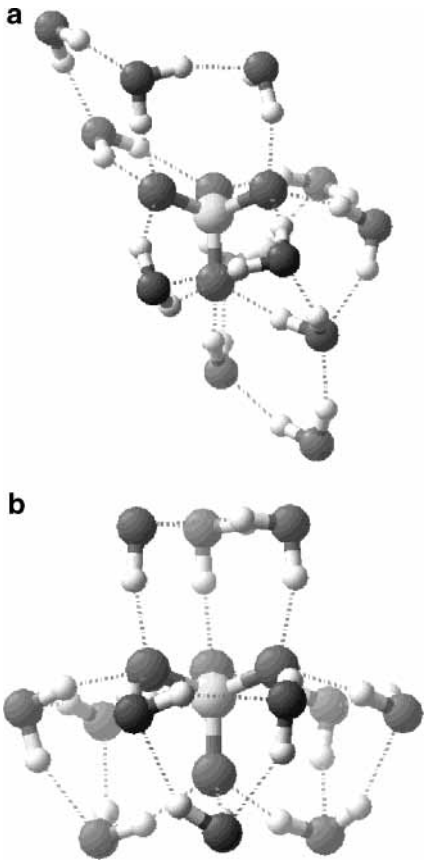

Figure 6. Possible structures of $SO_4^{2-}(H_2O)_{12}$ with (a) two water molecules in a second solvation shell and (b) all water molecules in the first solvation shell.

6b) is 12 kJ/mol higher in energy than the two-shell structure (Figure 6a). These results indicate that a 12 kJ/mol threshold may be too low to identify the lowest energy structures at the mechanics level, and that many structures are likely to be populated under the conditions of this experiment. These results also indicate that a structure in which all the water molecules are in the first solvation shell (Figure 6b) is at least energetically competitive with structures in which one or more water molecules are in the second solvation shell, although many more of the latter structures are likely to be energetically competitive.

$SO_4^{2-}(H_2O)_5$. A 4.0-s BIRD spectrum of $SO_4^{2-}(H_2O)_n$, $n = 5$, is shown in Figure 3c. Ions corresponding to mostly charge separation products and a very small peak corresponding to the $n = 4$ cluster are obtained. Since both $HSO_4^-(H_2O)_2$ and $OH^-(H_2O)_3$ appear in the spectrum, the $n = 5$ clusters must have dissociated through two independent charge separation reactions (reactions 5a and 5b).

$$SO_4^{2-}(H_2O)_5 \rightarrow HSO_4^-(H_2O) + OH^-(H_2O)_3 \quad (5a)$$

$$\rightarrow HSO_4^-(H_2O)_2 + OH^-(H_2O)_2 \quad (5b)$$

$$\rightarrow SO_4^{2-}(H_2O)_4 + H_2O \quad (5c)$$

In a separate experiment, $HSO_4^-(H_2O)$ is isolated and trapped in the ion cell at the same experimental conditions. No $HSO_4^-(H_2O)_2$ is obtained, confirming that the $HSO_4^-(H_2O)_2$ signal in Figure 3c is not due to an association reaction.

Because $SO_4^{2-}(H_2O)_5$ dissociates through three processes and because its products also subsequently dissociate, the branching ratios for reactions 5a, 5b, and 5c are difficult to obtained accurately. Nevertheless, a rough estimate can be made for these

reactions. By using the relative abundances of $OH^-(H_2O)_3$ to $OH^-(H_2O)_2$ in Figure 3c, the branching ratio between reactions 5a and 5b is determined to be at least 11:1. This ratio is a lower limit because $OH^-(H_2O)_3$ can subsequently dissociate to form $OH^-(H_2O)_2$. The abundance ratio of $HSO_4^-(H_2O)_2$ to $HSO^-(H_2O)$ doubles under the higher internal energy deposition obtained with SORI-CAD (Figure 3d versus Figure 3c). The maximum kinetic energy of $SO_4^{2-}(H_2O)_5$ during the SORI cycle is ~7.8 eV in the lab frame and ~1 eV in the center of mass frame. Although both fragment ions can subsequently lose a water molecule, this should occur more for $HSO_4^-(H_2O)_2$ than for $HSO_4^-(H_2O)$. Thus, these results indicate that reaction 5b is entropically favored over reaction 5a. This is consistent with fewer water molecules needing to be rearranged for reaction 5b. Blades and Kebarle have argued that reaction 5a is energetically favorable based on the relative stability of the product ions,[14] consistent with our energy dependence studies.

As will be shown in the next section, the $n = 4$ cluster dissociates to $OH^-(H_2O)_2$ but not $OH^-(H_2O)_3$. Assuming that all $OH^-(H_2O)_2$ ions in Figure 3c are formed from the $n = 4$ cluster, the abundance ratio of $[SO_4^{2-}(H_2O)_4 + OH^-(H_2O)_2]$: $[OH^-(H_2O)_3]$ represents an upper limit of 1:10 for the branching ratio between dehydration reaction 5c and charge separation reaction 5a. Formation of the $n = 4$ cluster can be significantly enhanced by using SORI-CAD (Figure 3d). The higher energy deposition from SORI-CAD dramatically increases the dehydration channel, which is only a very minor process with BIRD or IRMPD. Based on the assumption that the $n = 4$ cluster does not undergo subsequent dissociation, a lower limit of 3:10 is obtained to the dehydration reaction 5c to both charge separation processes for the SORI-CAD experiment (Figure 3d). This is over a 3-fold increase compared to BIRD. Note that most of the *m*/*z* 75 signal in Figure 3d is not the dianion $SO_4^{2-}(H_2O)_3$ but singly charged $CH_3OCO_2^-$ (see below). The BIRD and SORI-CAD experiments demonstrate that the dehydration reaction is favored at high internal energy, and that the charge separation reactions are favored at low internal energy. As one would expect, water molecule detachment from $SO_4^{2-}(H_2O)_5$ is entropically favored because it is a direct cleavage reaction (reaction 5c), and the charge separation processes of reactions 5a and 5b are energetically favored due in part to contributions of the columbic repulsion between the charged product ions.

Impurity at *m*/*z* 75. To identify the *m*/*z* 75 peak in Figure 3d, SORI-CAD was done and a single product ion at *m*/*z* 31 was formed, which corresponds to a loss of CO_2 from $CH_3OCO_2^-$. Due to carbonate ion ($CH_3OCO_2^-$) impurities, the $CH_3OCO_2^-(H_2O)_m$ peaks overlap with every other peak of $SO_4^{2-}(H_2O)_n$ when n is an odd integer. This contaminant was also observed by Blades and Kebarle, despite using different reagents. As will be shown later, care must be taken in forming the $n = 3$ ion to avoid interference from the $CH_3OCO_2^-$ impurity.

Except for the *m*/*z* 75 produced directly from *m*/*z* 93, the abundance of the $CH_3OCO_2^-(H_2O)_m$ is negligible compared to that of the $SO_4^{2-}(H_2O)_n$ (Figure 3d). As described earlier, the double resonance experiment showed that the $SO_4^{2-}(H_2O)_{13}$ (*m*/*z* 165) dissociates to a product ion at *m*/*z* 156, corresponding to the loss of a water molecule (Figure 2a−d). The isotope peaks confirm that these ions are doubly charged. Direct loss of 18 Da is not observed, which suggests that $CH_3OCO_2^-(H_2O)_{10}$ is low in abundance by comparison. Similar results are obtained for $SO_4^{2-}(H_2O)_n$, $n = 7-17$, clusters, indicating that $SO_4^{2-}(H_2O)_n$ signals are large compared to those from $CH_3OCO_2^-(H_2O)_m$ clusters. BIRD of the $n = 5$ ion (*m*/*z* 93) results in formation

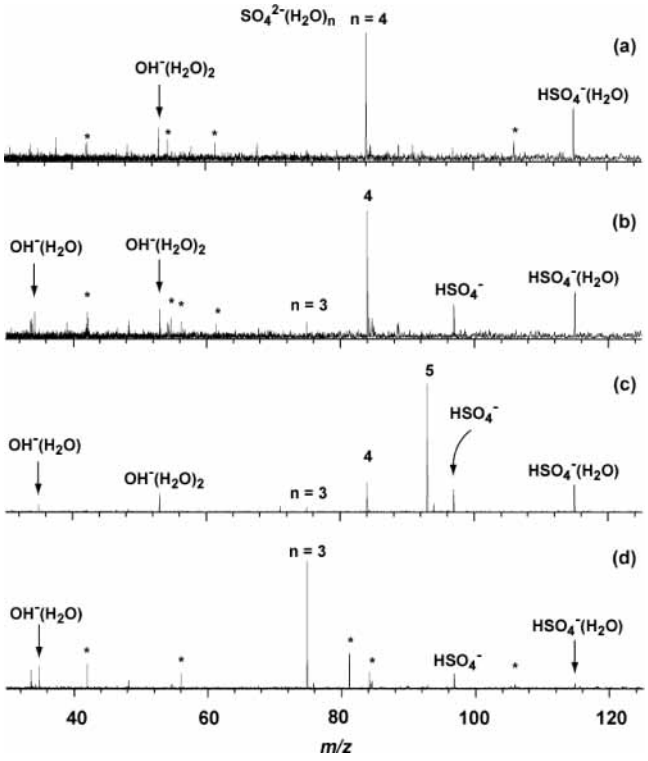

Figure 7. Dissociation spectra of (a) $SO_4^{2-}(H_2O)_4$ with BIRD (0.5 s, 21 °C), (b) $SO_4^{2-}(H_2O)_4$ with SORI-CAD, (c) $SO_4^{2-}(H_2O)_5$ with SORI-CAD (the $SO_4^{2-}(H_2O)_5$ ion was formed by IRMPD of $SO_4^{2-}(H_2O)_6$), and (d) $SO_4^{2-}(H_2O)_3$ with BIRD (0.02 s, 21 °C). Asterisks (*) indicate known noise peaks.

of $OH^-(H_2O)_2$ (*m*/*z* 53), $OH^-(H_2O)_3$ (*m*/*z* 71), $SO_4^{2-}(H_2O)_4$ (*m*/*z* 84), HSO_4^- (*m*/*z* 97), and $HSO_4^-(H_2O)$ (*m*/*z* 115), all of which are sensible product ions from $SO_4^{2-}(H_2O)_5$ and cannot be formed from $CH_3OCO_2^-(H_2O)$ (Figure 3c). Although $CH_3OCO_2^-(H_2O)$ comprises a very small fraction of the overall *m*/*z* 93 signal, its dissociation product $CH_3OCO_2^-$ (*m*/*z* 75) does not subsequently dissociate at low energy, whereas $SO_4^{2-}(H_2O)_3$ (*m*/*z* 75) does. Therefore, $CH_3OCO_2^-$ constitutes essentially all of *m*/*z* 75 ions dissociated from *m*/z 93 with SORI-CAD (Figure 3d).

$SO_4^{2-}(H_2O)_4$. Neither $SO_4^{2-}(H_2O)_n$, $n = 3$ or 4 is produced directly by electrospray ionization in these experiment. The $n = 4$ cluster is produced with SORI-CAD of the $n = 5$ cluster. The $n = 4$ cluster is then isolated and dissociated in a room temperature ion cell. The ion dissociates via a charge separation process (reaction 6; Figure 7a). The $n = 3$ cluster dissociates

$$SO_4^{2-}(H_2O)_4 \rightarrow HSO_4^-(H_2O) + OH^-(H_2O)_2 \qquad (6)$$

to form $HSO_4^-(H_2O)$ and $OH^-(H_2O)$ (see below). The lack of signals for $SO_4^{2-}(H_2O)_3$ (*m*/*z* 75) and $OH^-(H_2O)$ (*m*/*z* 35) in Figure 7a confirms that the charge separation process of reaction 6 is the dominant reaction. Because the $n = 4$ cluster ions are produced from $n = 5$ ions with SORI-CAD, the average internal energy of the $n = 4$ ions is higher than that of the surrounding ion cell. At room temperature, the charge separation reaction is expected to be more favorable than water elimination although the time scale for dissociation may be long. Similar results were obtained with IRMPD.

When the $n = 4$ cluster, which is produced from the $n = 5$ ion with SORI-CAD, is further activated with SORI-CAD, the dehydration process to $n = 3$ ion is enhanced (Figure 7b). The maximum kinetic energy of $SO_4^{2-}(H_2O)_4$ during the SORI-CAD

is ~14 eV in the lab frame and ~2 eV in the center of mass frame. Although the signal at *m*/*z* 75 is small, it is reproducibly formed. This observation was also reported by Blades and Kebarle.[14] Similar to the result for the $n = 5$ ion, the charge separation reaction for the $n = 4$ cluster is favored with use of low-energy activation methods, and the dehydration process is enhanced with use of higher energy SORI-CAD. These results confirm that the charge separation process is energetically favored, and the dehydration pathway is entropically favored.

$SO_4^{2-}(H_2O)_3$. Although the $n = 3$ cluster produced directly from the $n = 4$ cluster is free of $CH_3OCO_2^-$ impurity, the production of this ion by consecutive SORI-CAD of $n = 5$ and 4 clusters is inefficient. This is due to the dominance of the charge separation pathway for both the $n = 4$ and 5 clusters.

An alternative way of producing the $n = 3$ cluster is by depositing substantial energy into the $n = 5$ cluster without subsequent isolation and dissociation of the $n = 4$ ion. However, performing SORI-CAD on the $n = 5$ cluster directly obtained from electrospray ionization is not feasible because of the $CH_3OCO_2^-(H_2O)$ impurity problem described earlier. To obtain the $n = 5$ cluster free of $CH_3OCO_2^-(H_2O)$, the $n = 6$ cluster is isolated and dissociated to $n = 5$ with IRMPD. The resulting $n = 5$ ion is then isolated and dissociated to $n = 4$ and 3 ions by using SORI-CAD with high collisional energy (Figure 7c). The maximum kinetic energy of $SO_4^{2-}(H_2O)_5$ during the SORI cycle is ~62 eV in the lab frame and ~8 eV in the center of mass. Clusters corresponding to $n \leq 2$ are not observed during the "synthesis" of the $n = 3$ ion. Subsequent isolation and dissociation of the $n = 3$ ion in a room temperature ion cell results in charge separation products (reaction 7; Figure 7d).

$$SO_4^{2-}(H_2O)_3 \rightarrow HSO_4^-(H_2O) + OH^-(H_2O) \qquad (7)$$

Neither dehydration to form $SO_4^{2-}(H_2O)_2$ nor electron detachment to form $SO_4^-(H_2O)_n$ is observed. The $n = 3$ cluster produced via SORI-CAD is at higher internal energy than the surrounding room temperature. The $n = 3$ ion would be expected to undergo the energetically favored charge separation process in a 21 °C BIRD experiment, although the time scale for this process may be long. Due to its low intensity, the $SO_4^{2-}(H_2O)_3$ was not dissociated with SORI-CAD.

SO_4^-. In our experiments, no singly charged SO_4^- (*m*/*z* 96) was observed. Blades and Kebarle reported a product peak at *m*/*z* 96 from CAD of $SO_4^{2-}(H_2O)_4$,[14] and Wang and co-workers detected the same peak formed directly by electrospray ionization.[15] Both groups suggest that the peak at *m*/*z* 96 may be SO_4^- formed from SO_4^{2-} via electron detachment. Blades and Kebarle were surprised by the absence of $SO_4^{2-}(H_2O)$ in the spectrum, which they thought to be the precursor ion of SO_4^{2-} prior to electron detachment. Subsequent reports indicate that $SO_4^{2-}(H_2O)_n$, $n = 1$ and 2, are electronically unstable.[1,13,15−17] Thus, the electron detachment process might occur at higher order $SO_4^{2-}(H_2O)_n$ clusters producing singly charged $SO_4^-(H_2O)_n$, which subsequently dissociate to bare SO_4^-. On the other hand, the $n = 1$ and 2 clusters may have sufficient lifetimes due to the repulsive columbic barrier to become bare SO_4^{2-}. It is surprising that neither $SO_4^{2-}(H_2O)$ nor any $SO_4^-(H_2O)_n$ clusters have been observed as product ions in any experiments to date.

Conclusions

The dissociation of $SO_4^{2-}(H_2O)_n$ for $n = 3-17$ shows a change in fragmentation pathways from charge separation to form two singly charged ions for $n = 3$ and 4 to loss of a single water molecule for $n = 7-17$. For $n = 5$, the loss of a water molecule is <10% of the sum of two charge separation pathways whereas for $n = 6$, the loss of a water molecule is dominant (>90%). The energy dependence of the branching ratio of water loss to charge separation shows that the loss of a water molecule is entropically favored. BIRD rate constants for loss of a water molecule from $n = 6-17$ measured at 21 °C show a large increase between $n = 6$ and 7, and a "magic" number at $n = 12$. These results show that there is a very stable structure with six water molecules in the first solvation shell, which is consistent with the results from molecular modeling. The seventh water molecule either goes into the second solvation shell or may still be in the first solvation shell, but disrupts the unusually stable structure corresponding to six water molecules. Both types of structures are comparable in energy at the mechanics level. The magic number at $n = 12$ is consistent with the 13th water molecule entering the second solvation shell. A low-energy symmetrical structure in which all 12 water molecules each form one hydrogen bond to SO_4^{2-} and two hydrogen bonds to two adjacent water molecules is identified at the B3LYP 6-31 G**++ level. It is comparable in energy to a structure in which 2 of the 12 water molecules are in the second solvation shell, but the latter structure is energetically favored at 25 °C. In addition, many more two solvation shell structures appear to be energetically competitive.

Acknowledgment. The authors would like to acknowledge assistance from Professor Lai-Sheng Wang's group, especially Dr. Xin-Yang, for numerous helpful discussions. This research would not have been possible if not for the generous financial support provided by National Science Foundation (grant CHE-0098109).

References and Notes

(1) Boldyrev, A.; Simons, J. *J. Phys. Chem.* **1994**, *98*, 2298−2300.
(2) McKee, M. L. *J. Phys. Chem.* **1996**, *100*, 3473−3481.
(3) Blades, A. T.; Jayaweera, P.; Ikonomou, M. G.; Kebarle, P. *J. Chem. Phys.* **1990**, *92*, 5900−5906.
(4) Peschke, M.; Blades, A. T.; Kebarle, P. *Int. J. Mass Spectrom.* **1999**, *187*, 685−699.
(5) Hettich, R. L.; Compton, R. N.; Ritchie, R. H. *Phys. Rev. Lett.* **1991**, *67*, 1242−1245.
(6) Petrie, S.; Javahery, G.; Wang, J. R.; Bohme, D. K. *J. Phys. Chem.* **1992**, *96*, 6121−6123.
(7) Schnier, P. D.; Gross, D. S.; Williams, E. R. *J. Am. Chem. Soc.* **1995**, *117*, 6747−6757.
(8) Kaltashov, I. A.; Fabris, D.; Fenselau, C. C. *J. Phys. Chem.* **1995**, *99*, 10046−10051.
(9) Williams, E. R. *J. Mass Spectrom.* **1996**, *31*, 831−842.
(10) Wang, X. B.; Ding, C. F.; Wang, L. S. *Phys. Rev. Lett.* **1998**, *81*, 3351−3354.
(11) Ding, C. F.; Wang, X. B.; Wang, L. S. *J. Chem. Phys.* **1999**, *110*, 3635−3638.
(12) Wang, L. S.; Ding, C. F.; Wang, X. B. *Chem. Phys. Lett.* **1999**, *307*, 391−396.
(13) Whitehead, A.; Barrios, R.; Simons, J. *J. Chem. Phys.* **2002**, *116*, 2848−2851.
(14) Blades, A. T.; Kebarle, P. *J. Am. Chem. Soc.* **1994**, *116*, 10761−10766.
(15) Wang, X. B.; Nicholas, J. B.; Wang, L. S. *J. Chem. Phys.* **2000**, *113*, 10837−10840.
(16) Yang, X.; Wang, X. B.; Wang, L. S. *J. Phys. Chem. A* **2002**, *106*, 7607−7616.
(17) Wang, X. B.; Yang, X.; Nicholas, J. B.; Wang, L. S. *Science* **2001**, *294*, 1322−1325.
(18) Spears, K. G.; Fehsenfeld, G. C.; McFarland, M.; Ferguson, E. E. *J. Chem. Phys.* **1972**, *56*, 2562−2566.
(19) Spears, K. G.; Fehsenfeld, G. C. *J. Chem. Phys.* **1972**, *56*, 5698−5705.
(20) Beyer, M.; Williams, E. R.; Bondybey, V. E. *J. Am. Chem. Soc.* **1999**, *121*, 1565−1573.

(21) Stace, A. J. *J. Phys. Chem.* **2002**, *106*, 7993−8005.
(22) Caminiti, R.; Paschina, G.; Pinna, G.; Magini, M. *Chem. Phys. Lett.* **1979**, *64*, 391−395.
(23) Musinu, A.; Paschina, G.; Piccaluga, G. *Chem. Phys. Lett.* **1981**, *80*, 163−167.
(24) Caminiti, R.; Paschina, G. *Chem. Phys. Lett.* **1981**, *82*, 487−491.
(25) Caminiti, R. *Chem. Phys. Lett.* **1982**, *86*, 214−218.
(26) Caminiti, R. *Chem. Phys. Lett.* **1982**, *88*, 103−108.
(27) Cannon, W. R.; Pettitt, B. M.; McCammon, J. A. *J. Phys. Chem.* **1994**, *98*, 6225−6230.
(28) Jungwirth, P.; Curtis, J. E.; Tobias, D. J. *Chem. Phys. Lett.* **2003**, *367*, 704−710.
(29) Gross, D. S.; Williams, E. R. *J. Am. Chem. Soc.* **1995**, *117*, 883−890.
(30) Price, W. D.; Williams, E. R. *J. Phys. Chem. A* **1997**, *101*, 8844−8852.